On the Determination of the Friction-Caused Energy Losses and its Potential for Monitoring Industrial Tribomechanical Systems

Dragomir Miljanić
Vladimir Milovanovic (vladicka@kg.ac.rs)
University of Kragujevac Faculty of Engineering: Univerzitet u Kragujevcu Fakultet inzenjerskih nauka
https://orcid.org/0000-0003-3071-4728
Djordje Vukelić
Dragan Rakić
Branko Tadić

Research Article

Keywords: Friction coefficient, Energy losses, Steep plane, Euler, Linear rolling guide.

Posted Date: May 3rd, 2023

DOI: https://doi.org/10.21203/rs.3.rs-2844605/v1

Version of Record: A version of this preprint was published at The International Journal of Advanced Manufacturing Technology on September 16th, 2023. See the published version at https://doi.org/10.1007/s00170-023-12288-y.

Abstract

The paper refers to a new method to quantify the energy losses due to frictional effects and imperfections in contacts in the case of real industrial tribomechanical systems. Whereby energy losses represent an integral indicator of quality of the real industrial tribomechanical system, in terms of the characteristics of the contact element materials, geometric accuracy, and manufacturing and assembly errors. This paper presents a very complex theoretical model based on the differential equation of motion of a real tribomechanical system down a steep plane. The outputs of the theoretical model are exact mathematical expressions that define the current values of the coefficient of friction and the friction-caused energy losses. The measuring system enables the quantification of current values of the distance traveled per unit of time. Based on a series of experimentally determined values of distance traveled per unit of time, the values of energy losses of the real industrial tribomechanical system are determined using the developed theoretical model and the appropriate software support. The obtained results indicate a high reliability, a large potential and a wide range of possible applications of the proposed method.

1 Introduction

As is known, friction represents the resistance to relative motion, be it sliding, rolling or combined sliding-rolling motion, of a pair of surfaces of two bodies. Friction opposes the relative motion of the body. Friction, as a complex phenomenon, has been the subject of investigation by many researchers for more than 400 years. The friction coefficient represents the main characteristic of every tribological system [1].

Numerous studies have investigated factors that have an influence on friction coefficient values. Primarily, factors are materials [2, 3], load [4], surface roughness [5], sliding velocity [6, 7], sliding mode [8], coating [9], lubricant [10, 11], temperature [12], or their combinations [13, 14]. For all these studies many researchers used analytical [15, 16] and numerical approaches [17, 18], mostly focusing on the experimental, measurement and modeling methods [19, 20], or artificial neural network (ANN) model to predict the friction coefficient based on experimental investigation [21].

Having knowledge of friction coefficient values, is of utmost importance during the development, maintenance and optimization of contact pairs, which are to be implemented in industrial systems. Based on the analysis of literature sources and existing tribometer solutions, in accordance with ASTM and ISO standards, it can be concluded that measurement methods and devices significantly affect the reliability of measurement results.

By investigating the possibilities of designing reliable and economical solutions for tribodiagnostic equipment that provide high measurement accuracy in testing finished industrial products, such as linear guides, many researchers have investigated and published their solutions.

Sheng-Hao Xu et al. [22] propose an analytical calculation method for predicting the time-varying friction of the roller linear motion guide. The model is formulated considering the combined effect of the time-

varying contact load, contact area and lubrication viscosity variations between the roller and raceway. Soleimanian & Ahmadian [23] consider friction effects in pre-sliding and sliding regimes of lubricated linear roller guideway systems to provide a dynamic model of the machine tool element. They applied single harmonic excitation forces at low frequencies to the rail and measured the force and response signals.

Kwang-Je Oh et al. [24] developed a testbed to measure the friction force of the linear motion ball guide with preload, compare measured frictional forces with predicted values and analyze the friction force components. Krampert et al. [25] integrated sensors into a linear guide and implemented a method for capturing the load on a rolling element linear guide by measuring the stresses resulting from the rolling element contact at the side of the runner block. They also compared obtained measurements with analytical and finite element method simulation. Considering that linear guideways have predominantly replaced box ways in industrial machinery to facilitate linear directional motion, Whitican et al. [26] address the problem of guides' nonlinearity. They developed a fixture allowing a physical connection with a servo-hydraulic shaker and tested a model for studying the form of the nonlinearity using the acceleration surface method. The structure was instrumented with triaxial accelerometers, and various excitation regimes were attempted on the structure.

Based on the analysis of previous investigations, this study proposes a novel theoretical model for determination of kinetic friction coefficient and presents experimental results. The proposed method is based on measuring two fundamental physical quantities, i.e., the distance traveled between fixed sensors and the time detected by sensors when a body passes through its reaction zones while sliding or rolling down an inclined plane-based test rig. The advantage of the proposed method is that the measurement process does not introduce any excitation into the measuring system, which results in high measurement accuracy. Furthermore, the location of the entire measuring system outside the friction zone opens a wide range of possibilities in terms of reliable and economical design solutions for tribodiagnostic equipment, especially when it comes to tribological tests in a controlled environment, such as tests at high temperatures or tests in a vacuum.

2 Theoretical Basis

The first published theoretical research related to the determination of kinetic friction coefficient via the dynamic equation of motion for a body moving down an inclined plane was published by Leonard Euler in 1748 [27].

Unfortunately, it is safe to say that this method has not experienced a broader expansion in the scientific field, especially in the design field of modern tribodiagnostic equipment. Papers based on (or related to) Euler's research are mainly published in journals focused on physics education. One of a few papers based on Euler's idea to determine the kinetic friction coefficient using the differential equation of motion was published in a thematic journal in the field of tribology [28].

From theoretical, experimental and technological aspects, a significant advantage of the proposed method is that it relies on measuring the three fundamental physical quantities (i.e., the mass, time and distance travelled). Following Euler's idea, a group of authors have conducted research [29] that represents one of a few published experimental verifications of Euler's method for determining the kinetic friction coefficient. The team applying for the grant has upgraded Euler's theoretical model by considering the effects of air resistance force on measurement errors, which are not to be neglected at higher velocities and low friction coefficient values on an inclined plane.

The upgraded Euler's theoretical model, which is planned to be verified experimentally, is based on the measurement of time required for the body of mass m to travel the distance s down an inclined plane, as illustrated in Fig. 1.

In the case from Fig. 1, the differential equation of motion down an inclined plane is as follows:

$$ma = m\frac{dv}{dt} = mg\sin\alpha - \mu mg\cos\alpha - kv^2$$

1

.

The expression $F_w=kv^2$ represents the air drag force. Using the following relations between the derivations

$$\frac{dv}{dt} = \frac{dv}{ds}\frac{ds}{dt} = v\frac{dv}{ds}$$

2

,

we get the equation:

$$mv\frac{dv}{ds} == mg\sin\alpha - \mu mg\cos\alpha - kv^2$$

3

.

The coefficient k equals

$$k = \frac{1}{2}C\rho_w A$$

4

,

where: *C* is the drag coefficient, ρ_w is the air density, *A* is the front surface of the body. Integral of the Eq. (3) is as follows:

$$\int mvdv = \int mg\sin\alpha ds - \int \mu mg\cos\alpha ds - \int kv^2 ds$$

5

.

The solution (5) can be written in the following form:

$$\frac{1}{2}mv^2 = E_k = A\left(m\vec{g}\right) - A\left(\vec{F}_\mu\right) - A\left(\vec{F}_w\right)$$

6

,

where: E_k – kinetic energy of the body on an inclined plane, $A\left(m\vec{g}\right)$ – work done by the Earth's gravitational force in the direction of motion, $A\left(\vec{F}_\mu\right)$ – work done by the friction force, and $A\left(\vec{F}_w\right)$ – work done by the air drag force.

Work done by the Earth's gravitational force equals:

$$A\left(m\vec{g}\right) = mg\sin\alpha s$$

7

.

Work done by the friction force $A\left(\vec{F}_w\right)$, that is the energy E_μ spent on overcoming the friction force (Fig. 2) can be written in the following form:

$$A\left(\vec{F}_\mu\right) = E_\mu = \int mg\mu\cos\alpha ds = \int_0^s F_\mu(s)\,ds = \bar{\mu}mg\cos\alpha s$$

8

,

where $\bar{\mu}$ is the mean value of the friction coefficient on the distance *s*.

As stated above, the air drag force $\vec{F}_w$ depends upon the squared velocity. The general diagram of the change in velocity of the body on an inclined plane is given in Fig. 3. Work done by the air drag force $A\left(\vec{F}_w\right)$ can be written as:

$$A\left(\vec{F}_w\right) = \int kv^2 ds = k\bar{v}^2 s$$

9

,

where $\bar{v}$ is the average velocity of the body, which satisfies Eq. (9).

By integrating the Eq. (6), considering that $v = \frac{ds}{dt}$, we get an equation:

$$v = \frac{ds}{dt} = \sqrt{2g\sin\alpha - 2g\bar{\mu}\cos\alpha - \frac{2k}{m}\bar{v}^2}\sqrt{s}$$

10

.

Further integration is as follows:

$$\int \frac{ds}{\sqrt{s}} = \int \sqrt{2g\sin\alpha - 2g\bar{\mu}\cos\alpha - \frac{2k}{m}\bar{v}^2}\, dt$$

$$\left(2\sqrt{s}\right)^2 = \left(\sqrt{2g\sin\alpha - 2g\bar{\mu}\cos\alpha - \frac{2k}{m}\bar{v}^2}\, t\right)^2$$

$$s = \frac{1}{2}\left(g\sin\alpha - g\bar{\mu}\cos\alpha - \frac{k}{m}\bar{v}^2\right)t^2 + R_1$$

11

.

Here, R_1 (denoting the integration constant) is equal to zero, considering the initial conditions (for $v = 0$ and $s = 0$). Eq. (11) represents the distance function in the presence of resistance forces (friction and drag). If we consider an idealized case, where no resistance forces are acting on the body, equations (10) and (11) are defined by the following:

$$v = v_i = gt_i \sin\alpha$$

12

,

$$s = s_i = \frac{1}{2} g {t_i}^2 \sin\alpha$$

13

.

By dividing Eq. (10) by Eq. (12) and Eq. (11) by Eq. (13), we get equations (14) and (15):

$$\left(\frac{v}{v_i}\right)^2 = \left(1 - \bar{\mu}ctg\alpha - \frac{k}{mg\sin\alpha}\bar{v}^2\right)\left(\frac{t}{t_i}\right)^2$$

14

,

$$\left(\frac{s}{s_i}\right) = \left(1 - \bar{\mu}ctg\alpha - \frac{k}{mg\sin\alpha}\bar{v}^2\right)\left(\frac{t}{t_i}\right)^2$$

15

.

Equation (16) is obtained from the condition that a body moving down an inclined plane in the presence of resistance travels the same distance as a body moving down an inclined plane without resistance. Eq. (16) defines the relations between the times required for a body to travel the same distance in two considered cases

$$\left(\frac{s}{s_i}\right)\left(\frac{t_i}{t}\right)^2 = \left(1 - \bar{\mu}ctg\alpha - \frac{k}{mg\sin\alpha}\bar{v}^2\right)$$

16

.

Let us consider the time ratio $\frac{t_i}{t}$, in the case of the same distance travelled ($s = s_i$). If we know (measure) the time *t* for which the body travels the path s in the presence of resistance, then we also know the time ratio $\frac{t_i}{t}$ because the time t_i can be calculated from Eq. (13):

$$t_i = \sqrt{\frac{2s}{g\sin\alpha}}$$

17

.

If the time ratio $\frac{t_i}{t}$ is denoted by ξ_o and included in Eq. (16), then Eq. (18) is obtained under the condition $s = s_i$

$$\left(\frac{t_i}{t}\right)^2 = {\xi_0}^2 = 1 - \bar{\mu}ctg\alpha - \frac{k}{mg\sin\alpha}\bar{v}^2$$

18

.

If we start from Eq. (1) and divide it by the quantity $mg\sin\alpha$, we obtain the following:

$$\frac{\frac{dv}{dt}}{g\sin\alpha} = 1 - \bar{\mu}ctg\alpha - \frac{k}{mg\sin\alpha}\bar{v}^2 = \frac{a}{a_i}$$

19

.

Equation (19) is valid for any value of μ and v so that we can write $\frac{\frac{dv}{dt}}{g\sin\alpha} = \frac{a}{a_i} = \left(\frac{t_i}{t}\right)^2 = {\xi_0}^2$.

Now we can obtain the values of acceleration, velocity and distance travelled for the case of body motion down an inclined plane in the presence of friction and air resistance, using the system of equations (20):

$$\begin{aligned} a &= a_i\left(\frac{t_i}{t}\right)^2 = g\sin\alpha\,{\xi_0}^2, \\ v &= v_i\left(\frac{t_i}{t}\right)^2 = g\sin\alpha\,{\xi_0}^2 t, \\ s &= s_i\left(\frac{t_i}{t}\right)^2 = \frac{1}{2}g\sin\alpha\,{\xi_0}^2 t^2. \end{aligned}$$

20

By substituting the first two equations of the system of equations (20) into Eq. (19), we obtain the formula for calculating the coefficient of friction as a function of time, that is, as a function of sliding velocity, as follows:

$$\mu = tg\alpha\left(1 - {\xi_0}^2 - \frac{1}{2m}C\rho_w A\sin\alpha\,{\xi_0}^4 g t^2\right)$$

21

,

$$\mu = tg\alpha\left(1 - {\xi_0}^2 - \frac{1}{2mg\sin\alpha}C\rho_w A v^2\right)$$

22

.

After substituting a part of the Eq. (21) by the third equation from the system of equations (20), we get:

$$\mu = tg\alpha \left(1 - {\xi_0}^2 - \frac{1}{m} C \rho_w A {\xi_0}^2 s\right)$$

23

.

Based on expression (8) for the coefficient of friction μ, it is possible to determine the energy spent on friction as a function of the sliding distance:

$$E_\mu = A\left(\vec{F}_\mu\right) = \int_0^s F_\mu(s)\, ds = mg\cos\alpha \int_0^s \mu ds$$

24

.

In Eq. (24), we can substitute the friction coefficient by Eq. (23):

$$E_\mu = mg\cos\alpha \int_0^s tg\alpha \left(1 - {\xi_0}^2 - \frac{1}{m} C \rho_w A {\xi_0}^2 s\right) ds$$

25

,

taking into account that the inclination angle is constant during the experiment, we can write Eq. (25) in the following form:

$$E_\mu = mg\cos\alpha\, tg\alpha \int_0^s \left(1 - {\xi_0}^2 - \frac{1}{m} C \rho_w A {\xi_0}^2 s\right) ds$$

26

.

By integrating Eq. (26), we get the formula for calculating the energy spent on overcoming the friction force:

$$E_\mu = mg\sin\alpha \left[\left(1 - {\xi_0}^2\right) s - \frac{1}{2m} C \rho_w A {\xi_0}^2 s^2\right]$$

27

.

The developed theoretical model enables the determination of the physical- theoretical dependence, based on two measured values (sliding distance *s* and sliding time *t*) and experimental conditions – quantities. So, we can express coefficient of friction μ as function $\mu = \mu(m,\ C_w, \rho_w,\ A,\ \alpha, v, s, t)$.

Significant scattering of the friction coefficient μ that occurs during the measurement of friction force and normal load on any type of measuring instrumentation (from basic tribometer configurations to sophisticated tribometers) is caused by the process dynamics, measuring device errors and surface microgeometry.

2.1 Considering the case of α = π/2

If we multiply the Eq. (22) by $mg\cos\alpha$, we obtain the equation:

$$F_\mu = \mu mg\cos\alpha = mg\sin\alpha\left(1 - {\xi_0}^2 - \frac{1}{2mg\sin\alpha}C\rho_w A v^2\right)$$

28

.

If we consider the case $\alpha\ = \pi/2$, the friction force is $F_\mu = 0$, $sin\alpha = 1$, and, in the general case, it is valid that $mg \neq 0$. Then Eq. (28) becomes:

$1 - {\xi_0}^2 - \frac{1}{2mg\sin\alpha}C\rho_w A v^2 = 0$ or ${\xi_0}^2 = 1 - \frac{1}{2mg}C\rho_w A v^2$. (29)

From the first equation of the system (20) and for considering case $\alpha\ = \pi/2$ Eq. (29) is reduced to:

$${\xi_0}^2 = \frac{a}{g}$$

30

.

When we include the expression (30) for ${\xi_0}^2$ in (29), we get the following:

$$\frac{a}{g} = 1 - \frac{1}{2mg}C\rho_w A v^2$$

31

.

Considering that $a = dv/dt$, Eq. (31) becomes:

$$\frac{dv}{dt} = g\left(1 - \frac{1}{2mg}C\rho_w A v^2\right)$$

32

.

Equation (32) can be written in the following form:

$$\frac{dv}{1-\frac{v^2}{\frac{2mg}{C\rho_w A}}} = gdt$$

33

.

In the general case, the following expression has a constant value so that we can denote it by k_1:

$$k_1 = \sqrt{\frac{2mg}{C\rho_w A}}$$

34

.

Now, the expression (33) can be written as:

$$\frac{dv}{1-\left(\frac{v}{k_1}\right)^2} = \frac{-{k_1}^2 dv}{v^2-{k_1}^2} = gdt$$

35

.

The solution of the differential Eq. (35) is of the form:

$$v = k_1 \frac{1+e^{-\frac{2gt}{k_1}}}{1-e^{-\frac{2gt}{k_1}}}$$

36

.

The limit value of the velocity equals:

$$v_g = \lim_{t\to\infty} v = k_1 \lim_{t\to\infty} \frac{1+e^{-\frac{2gt}{k_1}}}{1-e^{-\frac{2gt}{k_1}}}$$

37

.

According to Eq. (34) $k_1 > 0$ and $k_2 = \frac{2g}{k_1}, \quad g > 0$ we can solve Eq. (37) for limit value of the velocity:

$$v_g = \lim_{t\to\infty} v = k_1 \lim_{t\to\infty} \frac{1 + e^{-k_2 t}}{1 - e^{-k_2 t}} = k_1 \lim_{t\to\infty} \frac{1 + \frac{1}{e^{k_2 t}}}{1 - \frac{1}{e^{k_2 t}}} = k_1 \lim_{t\to\infty} \frac{1 + \frac{1}{\infty}}{1 - \frac{1}{\infty}} = k_1 = \sqrt{\frac{2mg}{C\rho_w A}}$$

38

.

The obtained expression (38) for calculating the limiting velocity v_g is well-known from theoretical mechanics. It refers to the free fall of a body in the air, where, after reaching the limiting velocity, the body continues to move at a uniform (limiting) velocity. That indicates that an inclined plane of an arbitrary angle of inclination represents a general physical model of body movement.

2.2 Considering the case of the limiting velocity

To support the statement, that an inclined plane of an arbitrary angle of inclination represents a general physical model of body movement, let us consider the case of the limiting velocity of a body moving down an inclined plane in the presence of friction. We start from Eq. (28) and the conditions for the velocity to reach its limiting value ($0 < \alpha < \pi/2; F_\mu = 0$). From Eq. (29) it follows:

$$mg\sin\alpha \neq 0 \quad \Rightarrow \quad \frac{1}{2mg\sin\alpha} C\rho_w A v^2 = 1 - {\xi_0}^2$$

39

.

From the previous condition follows the expression for the calculation of the limiting velocity at which the friction force has zero value:

$$v = \sqrt{\frac{\left(1 - {\xi_0}^2\right) 2mg\sin\alpha}{C\rho_w A}}$$

40

.

The first solution of Eq. (40) refers to the state of rest at $\alpha = 0$ and $v = 0$. From Eq. (40) follows that $\mu = 0$ and ${\xi_0}^2 = 1$.

Depending on tribomechanical characteristics of the body, the quantity ${\xi_0}^2$ can have an infinite number of values. At very small values of the friction coefficient, the ${\xi_0}^2$ approaches value 1. Theoretically, it is a

case of sliding of ideally smooth surfaces which are inert in terms of mutual adhesive action. In real technical systems, there is an infinite number of contact pairs in which $0 < {\xi_0}^2 < 1$.

Changes in the friction coefficient and the velocity for three different values of the inclination angle are shown in Fig. 4. The parameter ${\xi_0}^2$ was determined experimentally.

At the moment of reaching the critical speed ($v = v_g$) the body continues its motion with constant acceleration:

$$a = gsin\alpha(1 - \xi_0^2)$$

41

.

This value of acceleration corresponds to the limiting velocity ($v = v_g$) at which the contact between the body and the ramp separates.

3 Experimental setup

The experimental research plan foresees the development and implementation of a dedicated device a laboratory set, which would enable the determination of the coefficient of friction and energy losses occurring in real industrial tribomechanical systems. The designed device is planned to enable tests of linear roller guides of the "RAIL-TROLLEY" type in a wide range of industrial velocity and load values typical for such tribomechanical systems in industry. in industry. Figure 5 shows a schematic representation of the implemented device.

Figure 5 gives schematic representation of a real industrial guideway (1) based along the ξ axis, forming a certain angle α with with the horizontal plane. The α angle can be selected from a certain range of values, thereby allowing testing with a wide range of speeds. The cart (2) rolls along the guideway (1). A platform (3) is attached to the cart (2) through which, using the guideway assembly, different levels of normal load and moments along ξ, η and ζ axis can be simulated.

Desired normal load levels are achieved through the cart and platform mass, as well as additional masses, which act at the center of gravity (CG) of the cart-and-platform rolling assembly. Desired moment load along the axes ξ and ζ is achieved via the additional masses "m" and coordinate values of ξ and ζ, refering to CG of additional masses (Fig. 5 detail S1-S1 and detail S2-S2). With appropriate technical solutions, it is possible to simulate the load along the ζ axis and the moment load along the η axis (Fig. 5 detail S2-S2).

The measurement setup of the device consists of a magnetic tape (4) located in the carrier (5) fixed to the platform (3), magnetic tape reader (sensor 6) based on the stationary part of the device structure and corresponding Arduino electronics (7) meant for data management and storage of experimentally obtained values of distance travelled "s" per unit of time, going from position A to position B – Fig. 5.

Loaded linear rolling guideway assembly initially starts moving from position "A" (Fig. 5). A relatively small value of inclined plane angle and small value of rolling friction force enable the guideway to be manually brought to initial position "A", without difficulties, even under substantial loading of the system. The forced stopping of the loaded guideway in position "B" is performed via mechanical and hydraulic shock absorbers (8).

The foregoing presentation referred to the analysis of the conceptual solution for the device (Fig. 5). Globally, considerations are being made for a device solution that would simulate conditions identical to those in exploitation of real industrial tribomechanical systems (such as linear rolling guideways), and that would enable quantification of energy losses via a measurement setup and the presented theoretical model. Whereby the energy losses could be quantified at different levels and different types of loading of the rolling guideway assembly.

A combination of normal load and moment load along one and/or multiple axes represents the general case of loading on a guideway operating in industrial manufacturing systems. The possibility of simulating the exploitation conditions on a real industrial system and quantification of energy losses has significant qualitative advantages over model simulations, primarily in terms of the reliability of obtained results. A method based on the inclined plane principle clearly opens up a wide range of possible programmes of experimental testing of real industrial guideways.

In the following presentation, the paper authors present basic characteristics of the preliminarily realized device intended primarily for experimental verification of the proposed method.

Figure 6 shows the CAD model of the developed device, while Fig. 7 presents a photograph of the device.

The first functional subassembly consists of a real industrial hardened and ground guideway assembly whose elements are a rail of type HGH30CA and length 2000 mm (Position 1) and a moving cart (Position 2). The rail (Position 1) is attached by a detachable connection to a steel rectangular tube (Position 3) of length 2500 mm and cross-section dimensions of 80x60x3 mm. In the center of the tube's side wall, two openings with a diameter of 20 mm were made at a certain distance, which are used to position the formed functional subassembly under a certain slope. A stable steel platform (Position 4) of mass m = 31.4 kg and overall dimensions of 400x200x50 mm, used to simulate the normal load on the linear guideway assembly is attached to the mobile cart.

Mechanical shock absorber (Position 5) is mounted to the anterior of the platform’s front wall. Rectangular magnetic tape carrier with length of 2000 mm and cross-section dimensions 20x15 mm and a T-groove safety channel (Position 6) is mounted to the side wall of the platform. Magnetic tape (Position 7) is attached along the T-groove channel using prescribed joining technology.

The second functional subassembly, consisting of two steel U-profiles, is formed by welding pipes with a cross-sections of 80x60x3 mm and of certain lengths, and 500 mm long steel plates with a cross-section of 100x10 mm (Positions 8 and 9). On the side walls of the pipes, openings with a diameter of 20 mm

were made at certain distances, which are used to connect the first and the second functional subassemblies and to form the required slope angle. The connection is made via threaded spindles with a diameter of 20 mm (Position 10) passing through 20 mm openings, and nuts (Position 11), thereby forming closed-frame shaped stable structure (Fig. 6). The constructed profiles are mounted to the device chassis (Position 13) via four 12 mm diameter openings on the U-profiles' plates, and 12 mm diameter screws (Position 11).

Final position is determined by a hydraulic shock absorber, attached to one of the U-profiles via the plate (Position 14). Position 15 determines the location of the sensor (magnetic tape reader), while Position 16 determines the location of Arduino control electronics meant for data management and storage of experimentally obtained values of distance travelled "s" per unit of time, by a guideway loaded with a desired load, in the entire range of movement speeds, from zero to the speed defined by the chosen inclination angle and the actual present forces of resistance.

4 Experimental results

Experimental research was performed primarily to verify the reliability of the presented theoretical model of the proposed method, that is, the reliability of the method when quantifying friction and energy dissipation parameters in real industrial tribomechanical systems. When it comes to tribological parameters, such as the coefficient of friction, the most effective indicator of the reliability of the method is a small dispersion of the obtained results with a large number of experiment repetitions.

Figure 8 shows experimerimental curves of distance as a function of time for 10 experiment repetitions in identical test conditions and ideantical contact loading. The same diagram also shows the theoretical curve of distance change with time according to Eq. (13).

Figure 9 and 10 show graphs of friction coefficient change as a function of velocity and graphs of energy spent on distance travelled for all 10 performed experiments. Curves were plotted according to equations (22) and (27).

5 Statistical analysis of experimental results

The presented theoretical-experimental method is based on the law of distance travelled change with time for a real tribomechanical system. The distance change law was defined by Eq. (20) within the chapter concerning theoretical considerations, whereby distance travelled in the presence of resistive force is defined as a product of theoretical distance (s_i) and the ratio of theoretical and real time (t_i/t). Experimental data processing was performed in the software package "STATISTICA" using the Gauss-Newton method of nonlinear regression. Eq. (20), derived from theoretical considerations chapter, was taken as a base function for experimental data processing. For the purpose of statistical analysis of experimental data, two constants (C1 and C2) were added to the Eq. (20), determined by the processing program itself. Hence, data processing was performed using base function given as:

$$s = C_1 \, s_i \left(\frac{t_i}{t} \right)^{C_2}$$

42

.

Thereby, the obtained values of constants point to the degree of agreement between the theoretical model and experimentally determined values of distance travelled per unit of time. By processing experimental data regarding the ten performed experiments, obtained values of constants were found to be very similar to theoretical ones (C_1 = 1; C_2 = 2 - Eq. (20)), and coefficients of correlation were close to 1. The following example of output results regarding one of the ten performed experiments shows exactly that (Fig. 11).

6 Discussion

Friction phenomenon and energy losses due to friction have represented a very lively research area for centuries [30], and still do nowadays [31]. Friction, as a complex phenomenon, has been the subject of investigation by many researchers for more than 400 years. The friction coefficient represents the main characteristic of every tribological system, as is given in more detail in the review of literature sources.

Authors of this paper have for years followed in the footsteps of nineteenth-century Euler's research results regarding kinetic friction [27] and published their own research, as can be seen in references [28, 29]. Whereby, the Euler's method was generalised in terms of possible application and upgraded in terms of experimental verification of the method [28, 32, 33]. This paper primarily presents the generalised theoretical model of an inclined plane, which includes the actually present drag, besides just friction. The presented theoretical model, through equations (23) and (27), enables the calculation of current values of friction coefficient and energy spent on overcoming friction resistance as a function of all relevant process parameters, whereby the ξ_0 factor is experimentally determined.

The ξ_0 factor represents a ratio between real time spent travelling down an inclined plane (in the presence of resistive friction forces and drag) and travell time without resistive forces present (the idealised case). Meaning that by only measuring two basic phisical quantities (distance and time) during the process of a body travelling, current values of friction coefficient and values of energy spent could be quantified. Whereby, partial levels of energy spent on overcoming frictional resistance and energy spent on overcoming drag would be exactly quantified as functions of velocity and other process parameters.

The realised device and applied measurement setup enable a large amount of experimental data or strings of distance travelled and time values to be obtained in a very short time period, order of a second, thereby achieving a very high level of reliability of the measurement method. It should be emphasized that the applied measurement setup does not introduce excitation or error into the measurement system, unlike the sensors used for quantification of resistive forces. The performed experimental studies,

statistical data processing and obtained results (diagrams in Figs. 8–10.) all point to the high reliability of the method.

7 Conclusions

In this paper, a method of experimental determination of kinetic friction coefficient of real industrial rolling guideways was presented. The method is based upon the principle of following the law of change in distance travelled with time, in the case of a loaded real industrial guideway travelling down an inclined plane (rail of the guide). This method enables the testing of real industrial tribomechanical systems with a simulation of different types of loading. The obtained results point to the high reliability of the proposed method and open up a whole spectre of possible applications, in terms of tribological parameter quantification for real tribomechanical pairs while simulating real load levels and types, which offers significant advantages in qualitative terms. Quantification of friction of coefficient and energy spent values can present a uniqe indicator of quality of the industrial tribomechanical pair itself. Therefore, this method can be used for quality grading of standard industrial linear guideways. The authors' future research directions will be focused on examining real industrial guideways under simulated combined load and moment loads along axes. Research will also be focused on the implementation of the method for testing real industrial guideways under simulated dynamic loads.

Declarations

Funding

This research was supported by the Ministry of Education, Science and Technological Development of the Republic of Serbia.

Conflicts of interest/Competing interests

The authors declare no conflict of interest and no competing interests.

Authors' contributions

All authors contributed to the study's conception and design. Dragomir Miljanić: conceptualization, resources, funding acquisition, and writing—review and editing. Vladimir Milovanović: methodology, investigation, validation, visualization, and writing—original draft. Djordje Vukelić: methodology, software, visualization, and writing—review and editing. Dragan Rakić: formal analysis, software, and supervision. Branko Tadić: conceptualization, methodology, project administration, writing—original draft, and supervision. All authors read and approved the final version of the manuscript.

References

1. Blau PJ (2001) The significance and use of the friction coefficient. Tribol Int 34(9):585–591. https://doi.org/10.1016/S0301-679X(01)00050-0
2. Nuruzzaman DM, Chowdhury MA (2013) Friction Coefficient and Wear Rate of Different Materials Sliding Against Stainless Steel. Int J Surf Eng Interdisciplinary Mater Sci (IJSEIMS) 1(1):33–45. http://doi.org/10.4018/ijseims.2013010103
3. Alaci S, Muscă I, Pentiuc ȘG (2020) Study of the Rolling Friction Coefficient between Dissimilar Materials through the Motion of a Conical Pendulum. Materials 13:5032. https://doi.org/10.3390/ma13215032
4. Diez-Ibarbia A, Fernandez-Del-Rincon A, Garcia P et al (2018) Assessment of load dependent friction coefficients and their influence on spur gears efficiency. Meccanica 53:425–445. https://doi.org/10.1007/s11012-017-0736-8
5. Ivkovic B, Djurdjanovic M, Stamenkovic D (2000) The Influence of the Contact Surface Roughness on the Static Friction Coefficient. Tribology in Industry 22(3–4):41–44. http://www.tribology.fink.rs/journals/2000/3-4/1.pdf
6. Chowdhurya MA, Nuruzzamana DM, Miaa AH, Rahamana ML (2012) Friction Coefficient of Different Material Pairs Under Different Normal Loads and Sliding Velocities. Tribology in Industry 3422(1):18–23. http://www.tribology.fink.rs/journals/2012/2012-1/3.pdf
7. Hwang YM, Chen CC (2020) Investigation of Effects of Strip Metals and Relative Sliding Speeds on Friction Coefficients by Reversible Strip Friction Tests. Metals 10:1369. https://doi.org/10.3390/met10101369
8. Harouz R, Lakehal A, Khelil K, Dedry O, Hashemi N, Boudebane S, DRY SLIDING FRICTION AND WEAR OF THE WC/TIC-CO IN CONTACT WITH AL2O3 FOR TWO SLIDING SPEEDS. FACTA UNIVERSITATIS Series (2022) Mech Engi-neering 20(1):37–52. https://doi.org/10.22190/FUME200310039H
9. Smolin AY, Filippov AV, Shilko E, V. FRICTION BEHAVIOR OF ALUMINUM BRONZE REINFORCED BY BORON CARBIDE PARTICLES (2021) FACTA UNIVERSITATIS Series: Mechanical Engineering 19(1):51–65. https://doi.org/10.22190/FUME201226013S
10. Otero JE, Ochoa E, de la Tanarro G, del López EC (2017) Friction coefficient in mixed lubrication: A simplified analytical approach for highly loaded non-conformal contacts. Adv Mech Eng 9(7):1–11. https://doi.org/10.1177/1687814017706266
11. Čípek P, Vrbka M, Rebenda D, Nečas D, Křupka I (2020) Biotribology of Synovial Cartilage: A New Method for Visualization of Lubricating Film and Simultaneous Measurement of the Friction Coefficient. Materials 13:2075. https://doi.org/10.3390/ma13092075
12. Chung JO, Go SR, Choi HB, Son TK (2020) Temperature dependence of friction coefficient and transfer film formation in organic friction materials containing different abrasive components. Industrial Lubrication and Tribology 72(4):483–489. https://doi.org/10.1108/ILT-10-2019-0427
13. Folle LF, Caetano dos Santos Silva B, Sousa de Carvalho M, Zamorano LGS, Coelho RS (2022) Evaluation of the Friction Coefficient for TRIP1000 Steel under Different Conditions of Lubrication,

Contact Pressure, Sliding Speed and Working Temperature. Metals 12:1299. https://doi.org/10.3390/met12081299

14. Wen Q, Liu M, Zhang Z, Sun Y (2022) Experimental Investigation into the Friction Coefficient of Ball-on-Disc in Dry Sliding Contact Considering the Effects of Surface Roughness, Low Rotation Speed, and Light Normal Load. Lubricants 10:256. https://doi.org/10.3390/lubricants10100256
15. Argatov II, Chai YS, AN ANALYTICAL APPROACH TO THE THIRD BODY MODELLING IN FRETTING WEAR CON-TACT: A MINIREVIEW (2021) FACTA UNIVERSITATIS Series: Mechanical Engineering 19(1):125–131. https://doi.org/10.22190/FUME210103018A
16. Cao H, Zhu M, Li B, Lu X, Li H, Guo M, Wu F, Xu Z (2022) Theoretical Study of the Friction Coefficient in the M-B Model. Coatings 12:1386. https://doi.org/10.3390/coatings12101386
17. El-Bahloul SA (2020) Pre-drilling Effect on Thermal Friction Drilling of Cast Aluminum Alloy Using Thermo-mechanical Finite Element Analysis. J Appl Comput Mech 6(Special Issue) 1371–1379. https://doi.org/10.22055/jacm.2020.34682.2455
18. Wei S, Wei H, Saxen H, Yu Y (2022) Numerical Analysis of the Relationship between Friction Coefficient and Repose Angle of Blast Furnace Raw Materials by Discrete Element Method. Materials 15:903. https://doi.org/10.3390/ma15030903
19. Afrasiabi M, Saelzer J, Berger S, Iovkov I, Klippel H, Röthlin M, Zabel A, Biermann D, Wegener K (2021) A Numeri-cal-Experimental Study on Orthogonal Cutting of AISI 1045 Steel and Ti6Al4V Alloy: SPH and FEM Modeling with Newly Identified Friction Coefficients. Metals 11:1683. https://doi.org/10.3390/met11111683
20. Evin E, Daneshjo N, Mareš A, Tomáš M, Petrovčiková K (2021) Experimental Assessment of Friction Coefficient in Deep Drawing and Its Verification by Numerical Simulation. Appl Sci 11:2756. https://doi.org/10.3390/app11062756
21. Khalaf AA, Hanon MM (2022) Prediction of Friction Coefficient for Ductile Cast Iron Using Artificial Neural Network Meth-odology Based on Experimental Investigation. Appl Sci 12:11916. https://doi.org/10.3390/app122311916
22. Xu SH, Cheng DJ, Zhang SW (2022) Analysis of friction fluctuations mechanism of a preloaded roller linear motion guide based on a new 5-DOF dynamic stiffness model. Measurement 190:110768. https://doi.org/10.1016/j.measurement.2022.110768
23. Soleimanian P, Ahmadian H (2021) Modeling friction effects in lubricated roller guideways using a modified LuGre model. J Vib Control 28:19–20. https://doi.org/10.1177/10775463211013922
24. Oh KJ, Khim G, Park CH, Chung SC (2019) Explicit modeling and investigation of friction forces in linear motion ball guides. Tribol Int 129:16–28. https://doi.org/10.1016/j.triboint.2018.07.046
25. Krampert D, Unsleber S, Janssen C, Reindl L (2019) Load measurement in linear guides for machine tools. Sensors 19(15):3411. https://doi.org/10.3390/s19153411
26. Whitican SM, Van Karsen C, Blough J (2019) : Towards the Development of a Model for Nonlinear Elements in Machine Tools. In: Kerschen, G. (eds.) Nonlinear Dynamics 2019, Conference

Proceedings of the Society for Experimental Mechanics Series, vol. 1, pp. 405–417. Springer, Cham https://doi.org/10.1007/978-3-319-74280-9_46

27. Zhuravlev VP (2013) On the history of the dry friction law. Mech Solids 48:364–369. https://doi.org/10.3103/S002565441304002X
28. Mihajlović G, Gašić M, Savković M, Mitrović S, Tadić B (2017) Vibroplatform modeling with allowance for tribological aspects. J Frict Wear 38:184–189. https://doi.org/10.3103/S1068366617030102
29. Vukelic D, Todorovic P, Simunovic K, Miljojkovic J, Simunovic G, Budak I, Tadic B (2021) A Novel Method for Determination of Kinetic Friction Coefficient using Inclined Plane. Tehnički Vjesn 28(2):447–455. https://doi.org/10.17559/TV-20201101051835
30. Euler L (1750) Sur le frottement des corps solides. Memories de l'academie des sciences de Berlin 4:122–132
31. Miljojković J, Kočović V, Luković M, Živković A, Šimunović K (2022) Development of a Modular Didactic Laboratory Set for the Experimental Study of Friction. Tehnički Vjesn 29(1):269–277. https://doi.org/10.17559/TV-20210925171045
32. Brzaković L, Kočović V, Mitrović S, Busarac N, Tadić B (2022) A method for determing of kinetic friction coefficient under dynamic loading conditions. Rom J Phys 67:905. https://rjp.nipne.ro/2022_67_9-10/RomJPhys.67.905.pdf
33. Brzaković L, Milovanović V, Kočović V, Šimunović G, Vukelić D, Tadić B (2022) Relation between Kinetic Friction Coefficient and Angular Acceleration during Motion Initiated by Dynamic Impact Force. Tehnički Vjesn 29(5):1622–1628. https://doi.org/10.17559/TV-20220408155435

Figures

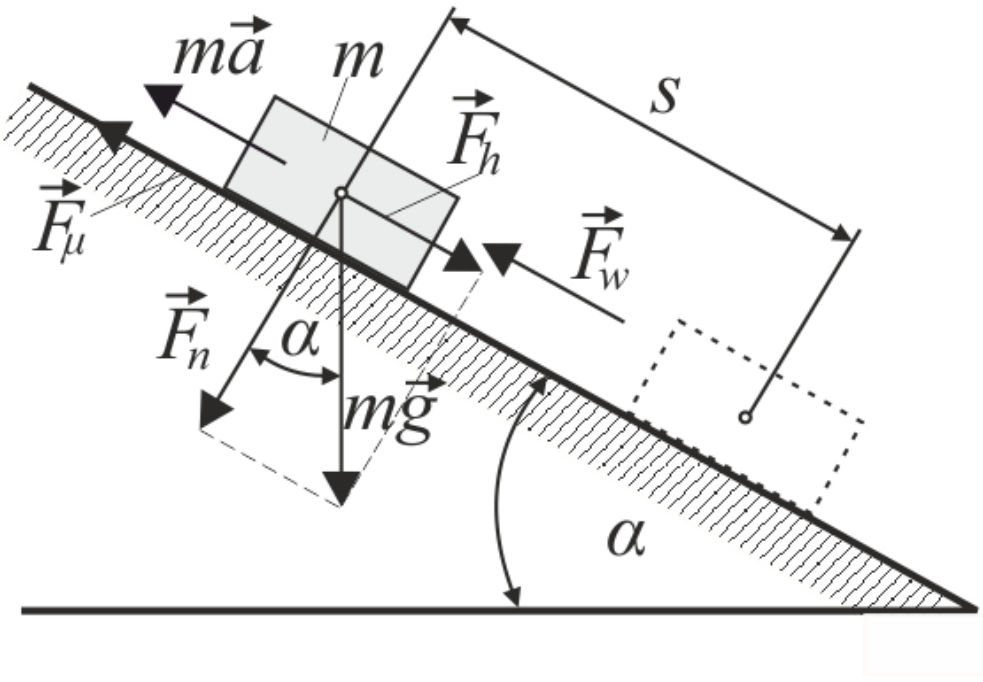

$$F_n = mg\cos\alpha$$
$$F_h = mg\sin\alpha$$
$$F_\mu = \mu F_n$$
$$F_w = kv^2$$

Figure 1

Motion of a body along an inclined plane – analysis of forces.

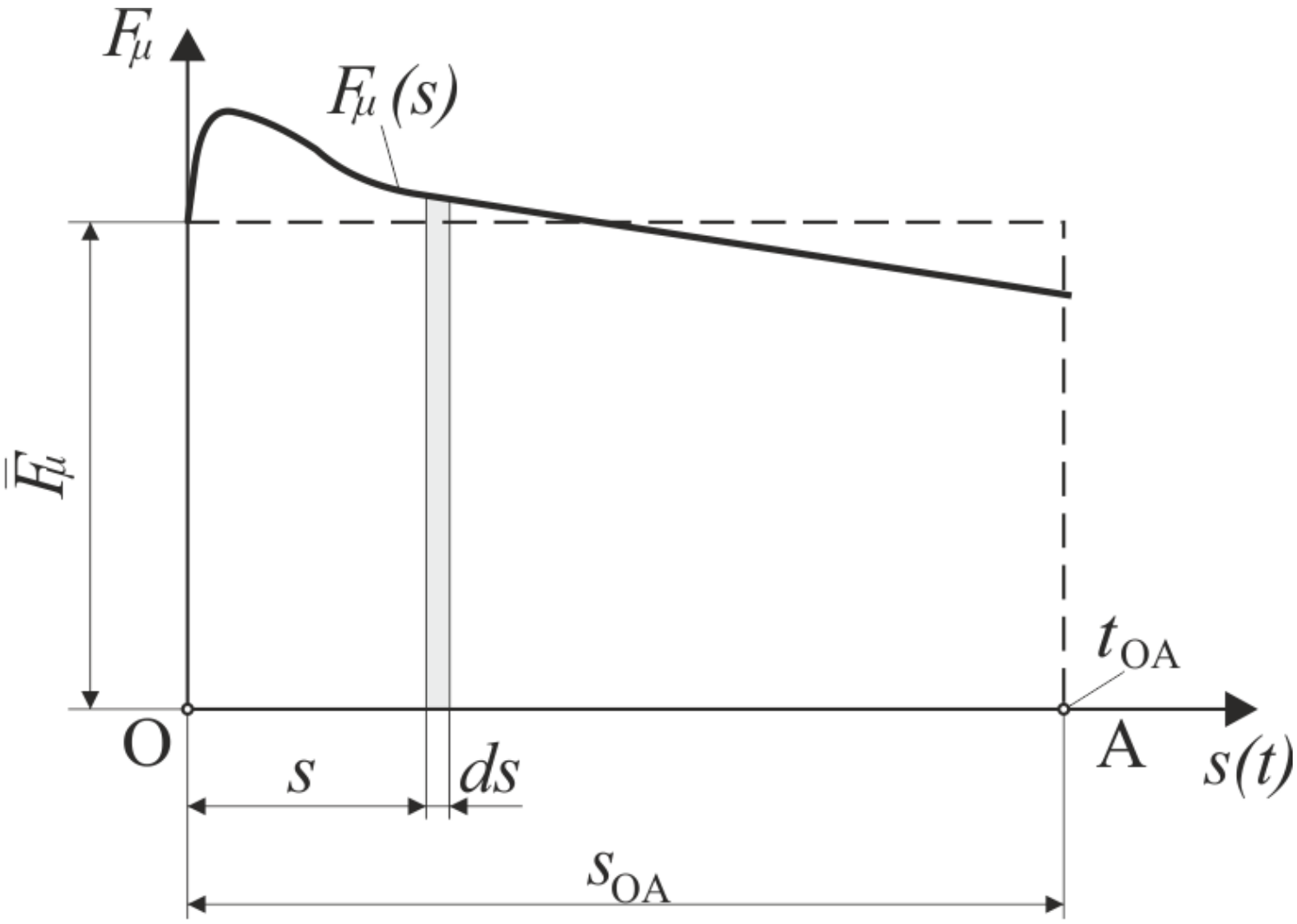

Figure 2

Work done by the friction force on the distance *s*.

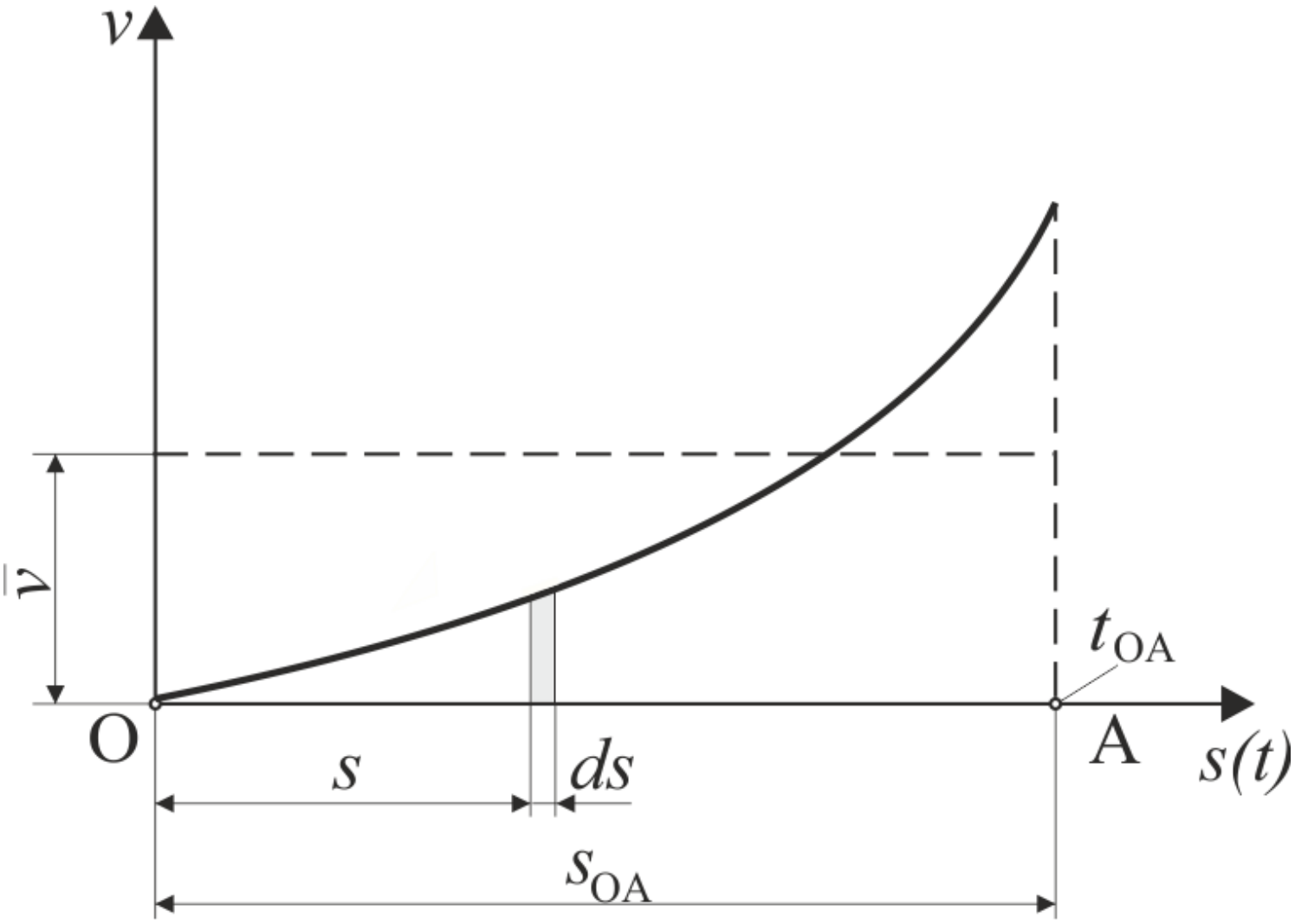

Figure 3

Change in velocity over time.

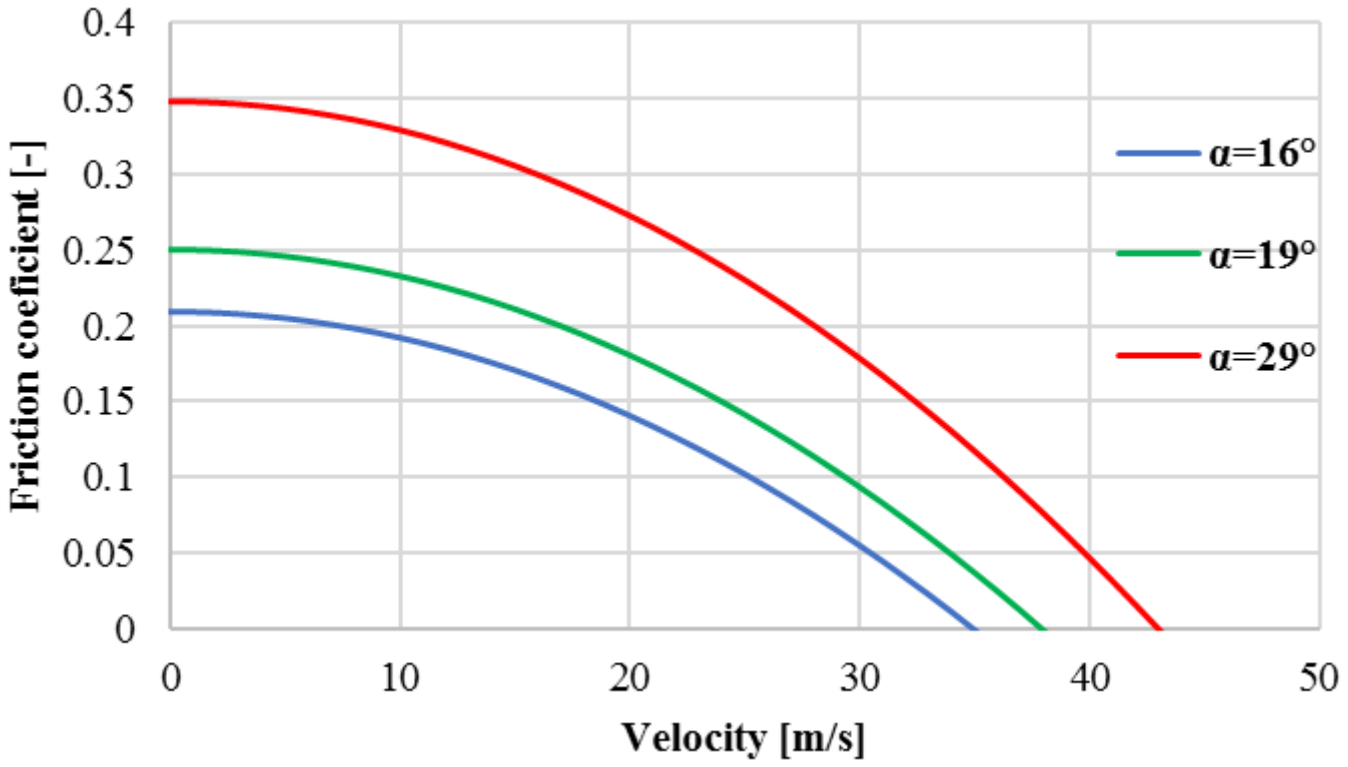

Figure 4

Changes in the friction coefficient depending on the velocity, for three different values of the inclination angle.

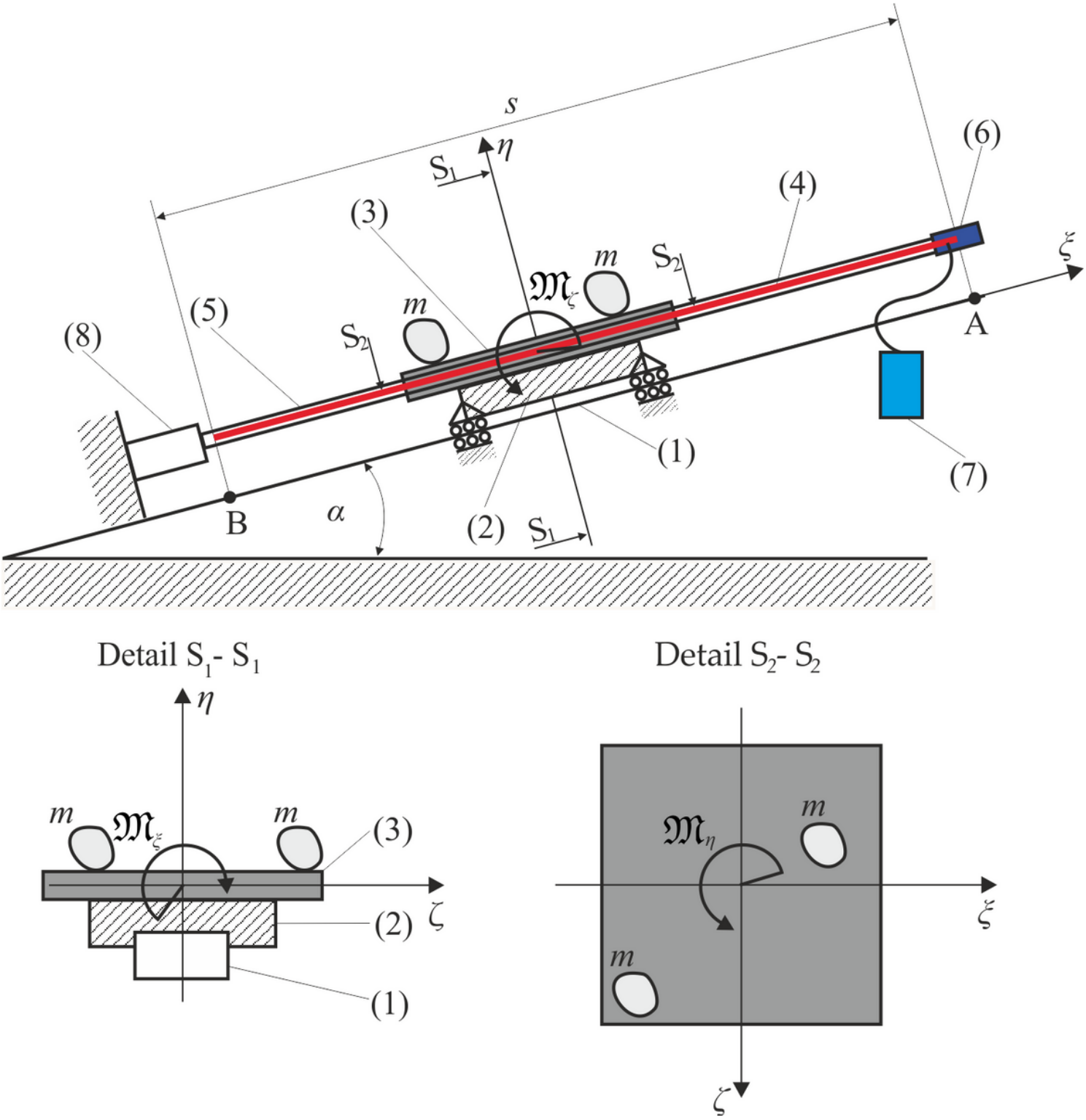

Figure 5

Schematic representation of the implemented device

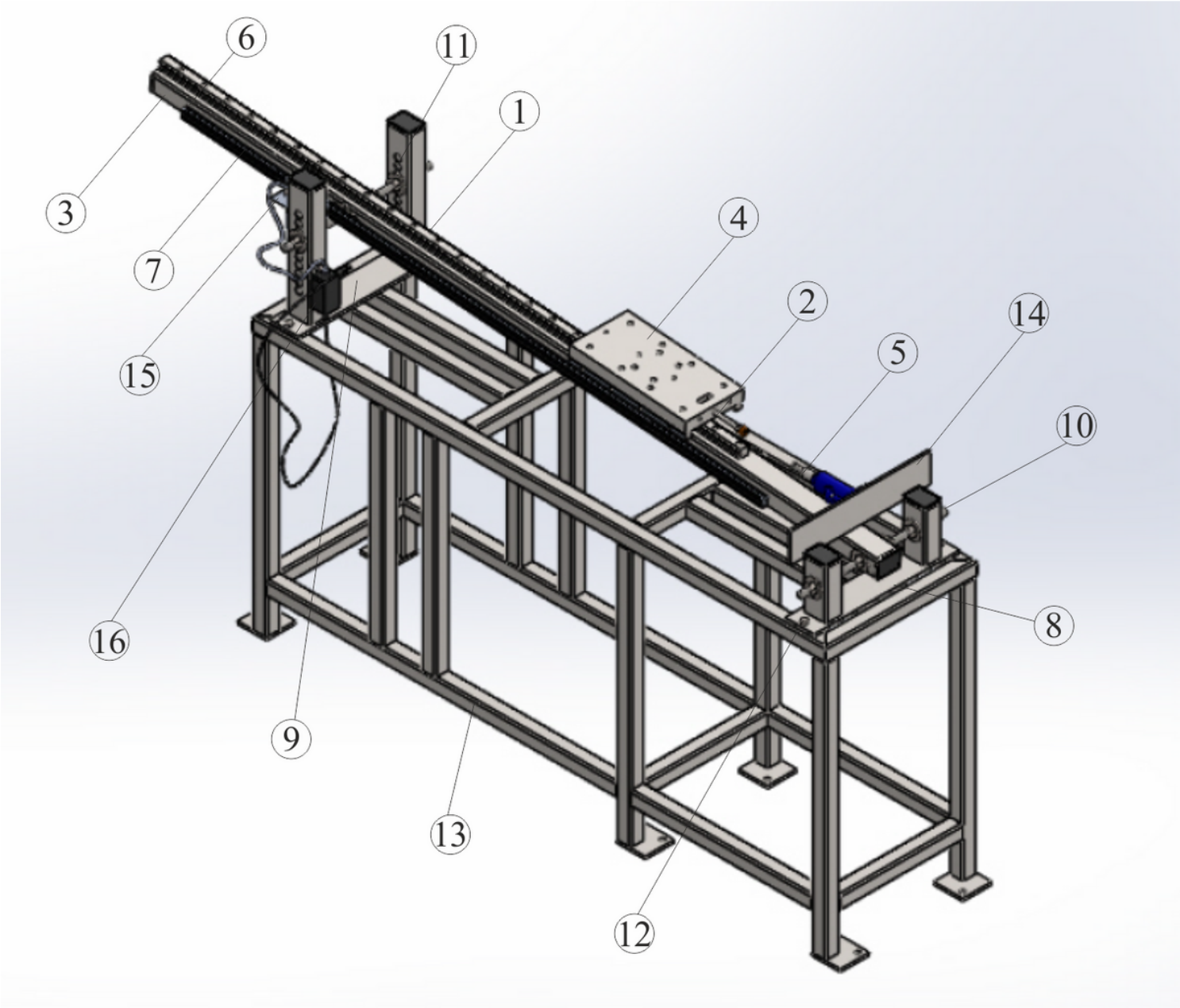

Figure 6

Isometric view of the device's CAD model

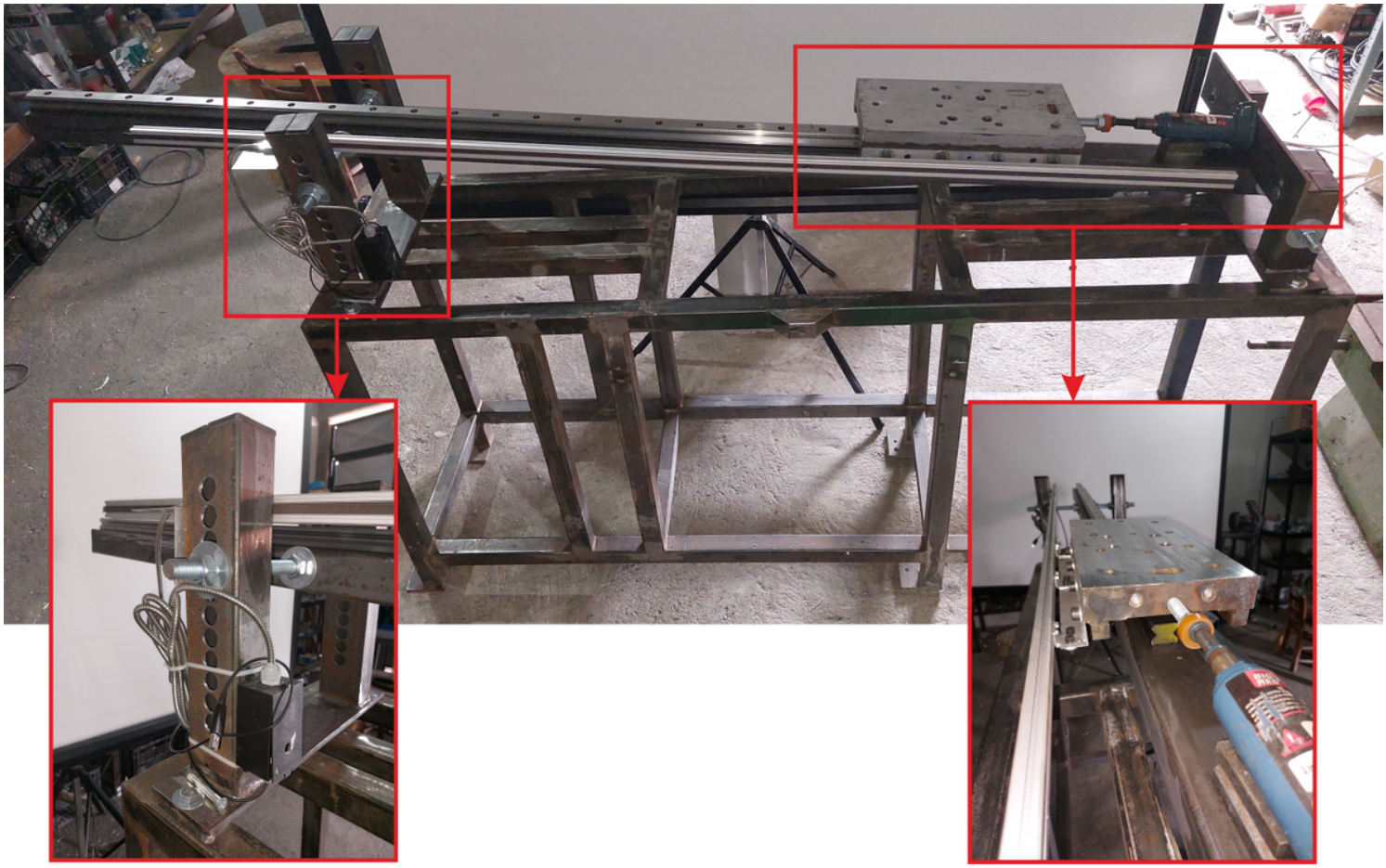

Figure 7

Photograph of the realized device

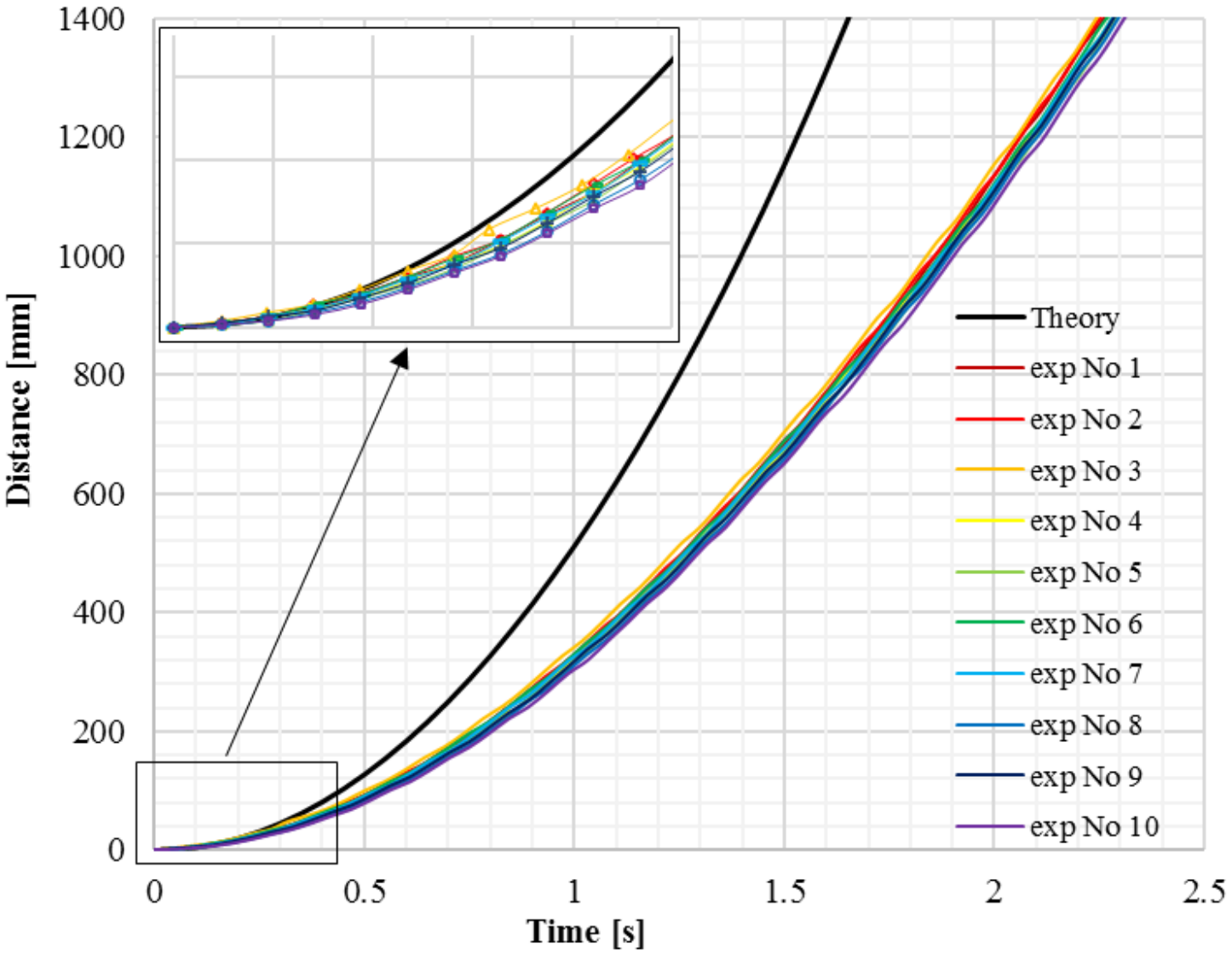

Figure 8

The theoretical curve of distance change with time and experimental curves of distance change with time in presence of the resistive friction force and drag.

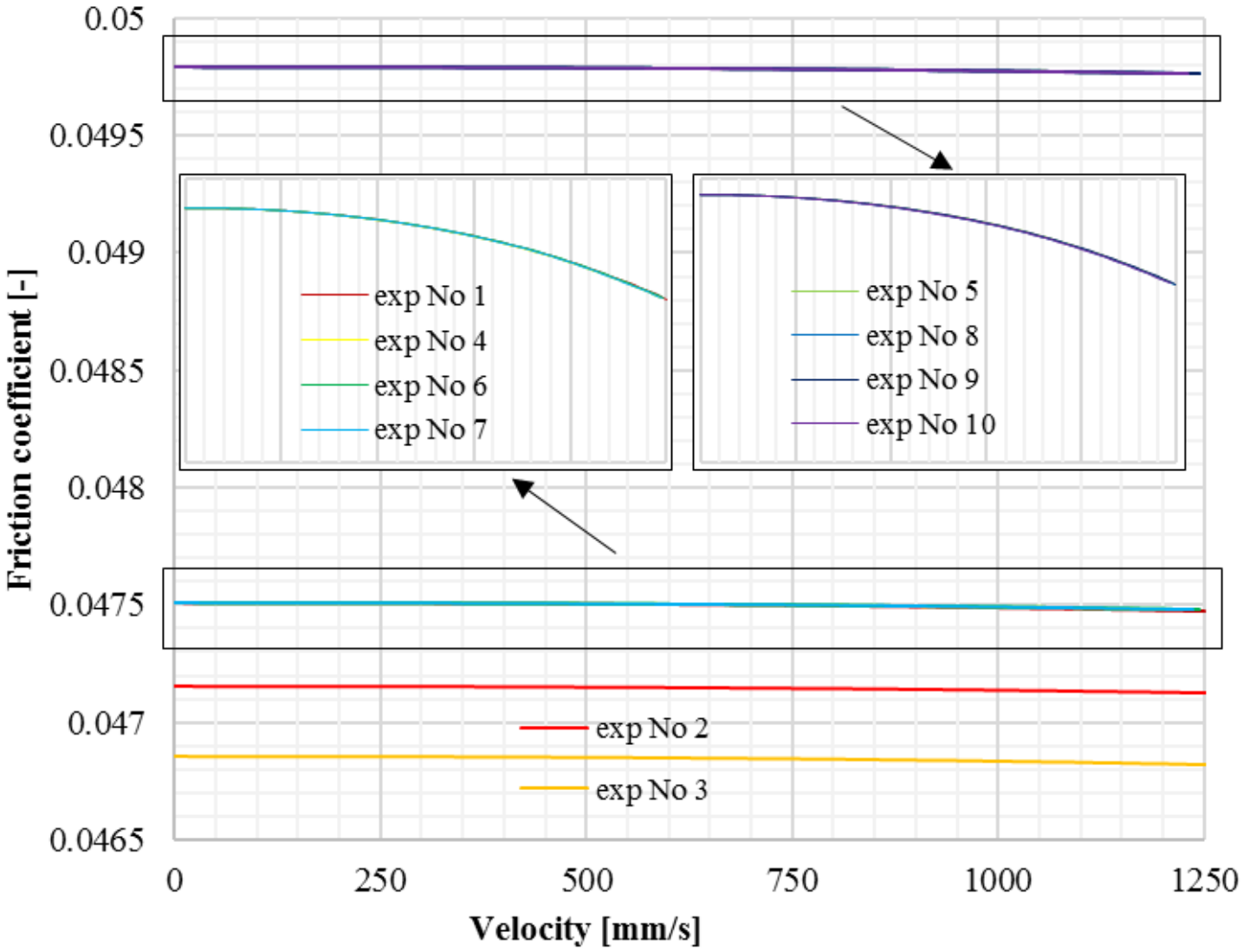

Figure 9

Experimental curves of the coefficient of friction change as a function of velocity.

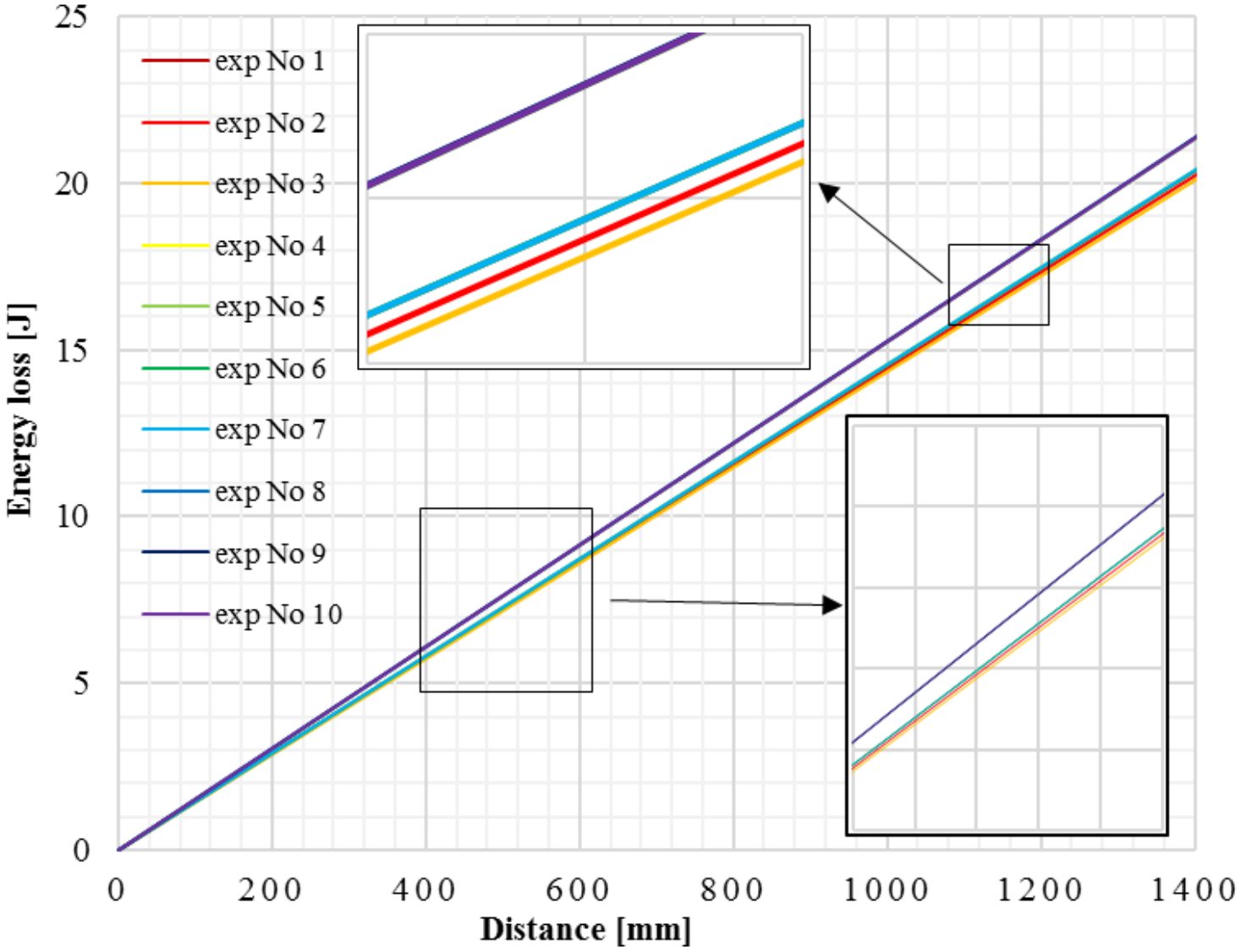

Figure 10

Experimental curves of energy spent (dissipated) on distance travelled.

S=C1*SI*KSI^(C2)

Dependent variable: S Independent variables: 2
Loss function: least squares
Final value: 0
Proportion of variance accounted for: 1 R =1

	Estimate	Standard error	t-value df = 47	p-level	Lo. Conf Limit	Up. Conf Limit
C1	0.999508	0.00	0.00	0.00	0.999508	0.999508
C2	2.000000	0.00	0.00	0.00	2.000000	2.000000

Figure 11

One example of output results displays from data processing in "STATISTICA" software package.